1-20-2017

Mechanistic understanding of ocean acidification impacts on larval feeding physiology and energy budgets of the mussel M. californianus

Matthew W. Gray

Chris J. Langdon

George G. Waldbusser

Burke Hales

Sean Kramer

Mechanistic understanding of ocean acidification impacts on larval feeding physiology and energy budgets of the mussel M. californianus

Article *in* Marine Ecology Progress Series · January 2017

DOI: 10.3354/meps11977

CITATIONS
3

READS
179

5 authors, including:

Matthew W Gray
University of Maryland Center for Environmental Science
38 PUBLICATIONS **222** CITATIONS
SEE PROFILE

Chris Langdon
Oregon State University
164 PUBLICATIONS **3,951** CITATIONS
SEE PROFILE

Burke Hales
Oregon State University
131 PUBLICATIONS **5,191** CITATIONS
SEE PROFILE

Vol. 563: 81–94, 2017
doi: 10.3354/meps11977

MARINE ECOLOGY PROGRESS SERIES
Mar Ecol Prog Ser

Published January 20

Mechanistic understanding of ocean acidification impacts on larval feeding physiology and energy budgets of the mussel *Mytilus californianus*

Matthew W. Gray[1,*], Chris J. Langdon[1], George G. Waldbusser[2], Burke Hales[2], Sean Kramer[3]

[1]Coastal Oregon Marine Experimental Station and Department of Fisheries and Wildlife, Hatfield Marine Science Center, Oregon State University, Newport, OR 97365, USA

[2]College of Earth, Ocean, and Atmospheric Sciences, Oregon State University, Corvallis, OR 97331, USA

[3]Department of Mathematics, College of Science & Mathematics, Norwich University, Northfield, VT 05663, USA

ABSTRACT: Ocean acidification (OA) — a process describing the ocean's increase in dissolved carbon dioxide (pCO_2) and a reduction in pH and aragonite saturation state (Ω_{ar}) due to higher concentrations of atmospheric CO_2 — is considered a threat to bivalve mollusks and other marine calcifiers. While many studies have focused on the effects of OA on shell formation and growth, we present findings on the separate effects of pCO_2, Ω_{ar}, and pH on larval feeding physiology (initiation of feeding, gut fullness, and ingestion rates) of the California mussel *Mytilus californianus*. We found that elevated pCO_2 delays initiation of feeding, while gut fullness and ingestion rates were best predicted by Ω_{ar}; however, pH was not found to have a significant effect on these feeding processes under the range of OA conditions tested. We also modeled how OA impacts on initial shell development and how feeding physiology might subsequently affect larval energy budget components (e.g. scope for growth) and developmental rate to 260 µm shell length, a size at which larvae typically become pediveligers. Our model predicted that Ω_{ar} impacts on larval shell size and ingestion rates over the initial 48 h period of development would result in a developmental delay to the pediveliger stage of >4 d, compared with larvae initially developing in supersaturated conditions ($\Omega_{ar} > 1$). Collectively, these results suggest that predicted increases in pCO_2 and reduced Ω_{ar} values may negatively impact feeding activity and energy balances of bivalve larvae, reducing their overall fitness and recruitment success.

KEY WORDS: Ocean acidification · Feeding · Scope for growth · Larva · Physiology · *Mytilus californianus*

INTRODUCTION

Oceanic uptake of anthropogenic carbon dioxide is altering the ocean's carbonate chemistry, acidifying the chemical environment and shifting the system towards more thermodynamically corrosive conditions for calcium carbonate — a process known as ocean acidification (OA; Doney et al. 2009). Developing prodissoconch bivalve larvae are especially sensitive to OA, and Waldbusser et al. (2015a,b) showed that initial shell development and growth are negatively affected as the aragonite saturation state (Ω_{ar}) approaches or falls below 1. OA effects on larval growth and development are due to the inability of early larvae to isolate shell-forming extra-pallial fluid from acidified seawater (Waldbusser et al. 2013), the high kinetic constraints on rapid calcification rates of initial shell formation (Waldbusser et al. 2013, 2015a,b), and allocation of limited, egg-derived, energy reserves for maintenance of cellular homeostasis (Stumpp et al. 2011, Timmins-Schiffman et al. 2013, Pan et al. 2015). In light of the increased energetic demands that OA imposes on developing larvae, investigations on energy acquisition and budgets are needed to better un-

*Corresponding author: matthew.gray@maine.edu

derstand how these commercially and ecologically important species respond to OA conditions.

Recently, studies have shown that larval invertebrate feeding and digestive functions are disrupted under OA conditions (Stumpp et al. 2013, Vargas et al. 2013). Reductions in feeding rates and digestive efficiencies will limit energy availability for energetically intensive processes like calcification and would likely impair development to the next life-stage. For mussel larvae, developmental delays have dire ecological consequences, as they promote greater exposure to pelagic planktivores and increase the likelihood of advection from likely favorable parental habitats (Rumrill 1990).

In this study, we explored the effects of acute OA exposure on the feeding physiology of the California mussel *Mytilus californianus* Conrad, 1837 and modeled how these physiological impacts might affect growth to the pediveliger life stage. To provide a mechanistic understanding of the impacts of OA on the feeding physiology of larvae, we hatched and incubated *M. californianus* larvae in a set of seawater treatments designed to separate the effects of 2 individual components of the marine carbonate chemistry system: the partial pressure of dissolved CO_2 (pCO_2) and aragonite saturation state (Ω_{ar}). The objectives of this study were (1) to determine the separate effects of pCO_2, Ω_{ar}, and pH on initiation of feeding, gut fullness, and ingestion rates of *M. californianus* larvae during the first 48 h of development; and (2) to model how the impacts of this acute OA exposure on larval feeding physiology may affect growth to the pediveliger life stage.

MATERIALS AND METHODS

We examined several parameters of the feeding physiology of *Mytilus californianus* larvae in response to different seawater carbonate chemistry parameters. Our study was based on measurements of larvae from the same spawn as those used in developmental and respiration experiments reported by Waldbusser et al. (2015b). We utilized a unique chemistry framework to fully separate the effects of pCO_2 and Ω_{ar} on developing larvae. This was accomplished by chemically manipulating the ratio and total quantities of total dissolved inorganic carbon and alkalinity, allowing pCO_2 and Ω_{ar} to vary independently of one another in a fully factorial design (Table 1). Responses to pH were partially correlated with pCO_2 and Ω_{ar}, as true independence of this factor only occurred within a subset of the experimental treatment matrix.

Chemical manipulations

Chemical manipulations of seawater to create experimental OA conditions were similar to those of Waldbusser et al. (2015b). Briefly, seawater was pumped at high tide from Yaquina Bay, Oregon, to the Hatfield Marine Science Center (HMSC) and filtered to 1 µm. Trace metal grade HCl (34 to 37%) was added to the collected seawater at near alkalinity equivalence, and the acidified seawater bubbled with ambient air to purge it of dissolved inorganic carbon (DIC). Water was then transferred to 20 l carboys, pasteurized, and stored at 2 to 5°C. Customized, gas-impermeable bags (EVOH-lined; Sholle Packaging) were filled with this treated seawater and immediately refrigerated at 2 to 5°C until experimental use (approx. 1 wk). To create OA seawater treatments, mineral acids and bases were added to the decarbonated seawater in the bags to achieve desired pCO_2 and Ω_{ar} values. At the beginning of the experiment, seawater from each treatment was transferred to 3 replicate 500 ml biological oxygen demand (BOD) bottles and warmed to 18°C. Antibiotics were added (10 ppm ampicillin and 2 ppm chloramphenicol) to the bottles to reduce bacterial activity.

Two control treatments were used in these experiments. Control 1 contained seawater that was collected at the same time as the water used for decarbonation, which was then 1 µm-filtered and immediately stored at 2 to 5°C to control for the effects of our chemical manipulations. Control 2 contained filtered seawater collected a day prior to the commencement of the experiment, which was 1 µm-filtered and aerated with CO_2-stripped (soda lime) air for 24 h as a control for larval development in newly collected seawater. Larvae from Control 1 were reared in volatile organic analysis (VOA; VWR) vials for initiation of feeding experiments while larvae from Control 2 were reared in open 10 l polyethylene aquaria and used as controls in particle processing experiments.

Larval rearing

Broodstock of *M. californianus* were collected from intertidal rocks of Seal Rock (44.7472° N, 124.0615° W) on the central Oregon Coast, a region which is seasonally exposed to upwelling of naturally 'acidified' water (Feely et al. 2008, Barton et al. 2012). Adult *M. californianus* broodstock were held under ambient conditions (10 to 14°C) at HMSC, fed continuously on an algal diet (*Chaetoceros* sp. and *Isochrysis galbana*), and spawned within 1 wk of collection.

Table 1. Carbonate chemistry of experimental treatments. Aragonite saturation state (Ω_{ar}) is reported over partial pressure of dissolved carbon dioxide (pCO_2) in µatm. Treatment pH (in parentheses) is expressed in the total scale. The control treatment consisting of freshly collected seawater that was bubbled with CO_2-reduced air for 24 h (Control 2), had values of Ω_{ar} = 3.25, pCO_2 = 272, and pH = 8.19. Experimental temperature and salinity were 18°C and 31, respectively. For dissociation constants used for computing the complete carbonate chemistry, we used Millero (2010) for the carbonic acid dissociation with water temperature and salinity dependencies, Dickson (1990) for constants for the dissociation of boric acid, and Millero (1995) for water dissociate constants

		Ω_{ar}			
		Low	MedLow	MedHigh	High
pCO_2	Low	0.50 / 219.0 (7.84)	1.09 / 197.4 (8.03)	1.87 / 241.5 (8.11)	4.58 / 191.1 (8.35)
	MedLow	0.31 / 715.7 (7.48)[a]	1.03 / 437.4 (7.84)	2.36 / 396.3 (8.04)	4.82 / 385.4 (8.21)
	MedHigh	0.51 / 873.8 (7.54)	1.17 / 773.7 (7.75)	2.33 / 803.5 (7.88)	4.69 / 767.6 (8.05)
	High	0.65 / 2228 (7.39)	1.31 / 2175 (7.55)	2.18 / 2457 (7.64)	5.21 / 2063 (7.86)

[a]There was a preservation problem in this treatment which caused pCO_2 to be greatly elevated relative to the initial treatment

Broodstock were stimulated to spawn by placing them in 10°C water-baths and rapidly increasing water temperature to 25°C. Although we attempted to spawn many individuals (>20), only 2 females and 2 males released their gametes during the spawning effort. Equal amounts of eggs were held separately in beakers and fertilized with sperm from different males to facilitate equal genetic contribution. After polar bodies were observed, embryos were rinsed of excess sperm, combined, and resuspended before being stocked in culture vessels in triplicate for each seawater treatment. For initiation of feeding experiments, larvae were cultured in 25 ml air-tight VOA vials to prevent any gas exchange and loss of treatment conditions. For all other feeding experiments, larvae were stocked in 500 ml BOD bottles, capped, and placed on their sides for 48 h at a culture temperature of 18°C (Bayne et al. 1976). We found seawater carbonate chemistry parameters to be well preserved during static egg incubations under these conditions, with pCO_2 increasing by ~10 to 30% after 48 h of incubation (Waldbusser et al. 2015a). Although we were unable to sample carbonate chemistry of VOA vials due to their small volumes, we assumed a similar small change in seawater carbonate chemistries because the eggs were incubated under similar conditions as those of BOD bottles. After 48 h of incubation, 3 subsamples were taken from each BOD bottle and preserved in 20 ml sample vials with addition of 10% buffered formalin (pH 8.1 to 8.2) for later determination of larval development and size, as reported by Waldbusser et al. (2015b). The remaining larvae were used for both respiration measurements (reported by Waldbusser et al. 2015b) and particle processing studies, presented here.

Feeding experiments

In all feeding experiments, we used polystyrene beads as surrogates for algal cells. The bead size chosen for these experiments was based on the findings of Baldwin & Newell (1995), who determined that early oyster *Crassostrea virginica* larvae preferentially ingested particles ranging from 1 to 3 µm in size. Fluorescent beads have been used as analogs for microalgae in feeding studies for a wide range of aquatic invertebrate taxa, including bivalve larvae (Solow & Gallager 1990, Thompson et al. 1994, Gray et al. 2015), ciliates (Pace & Bailiff 1987), freshwater and marine copepods (DeMott 1988), echinoderm larvae (Hart 1991), mosquito larvae (Dadd 1971), and rotifers (Armengol et al. 2001). Larval bivalve feeding rates obtained using beads have been found to be within the range observed in studies that rely solely on algae as food items (Widdows et al. 1989, Thompson et al. 1994, Gray et al. 2015). Fluorescent beads also possess useful qualities absent in natural algal diets because they are (1) inert and will not react chemically with experimental conditions, (2) uniform in shape, size, and surface characteristics, (3) easily visible and can be enumerated in the translucent larvae under an epifluorescent microscope, (4) can be stored without long-term loss of fluorescence, and (5) have the same specific gravity as algal cells (Milke & Ward 2003). We acknowledge, however, that beads lack the surface characteristics and nutritional content of algal cells, which may affect some feeding processes of bivalve larvae (Thompson et al. 1994, Espinosa et al. 2009).

Initiation of feeding

Impacts of water treatments on development of larval particle feeding mechanisms were determined by measuring the proportion of mussel larvae from each treatment that ingested fluorescent beads at 44 h post-fertilization (initiation of feeding, IF). Preliminary experiments demonstrated that at 44 h after fertilization, >50% of *M. californianus* larvae began feeding when reared at ambient pCO_2 (~380 ppm) and 18°C.

Waldbusser et al. (2015b) reported that initiation of feeding of *M. californianus* larvae was delayed by high pCO_2 (Fig. 1a). Here, we expand upon these findings and determine the length of the delay of the onset of feeding and how this delay affected the modeled growth of larvae to 260 µm in shell length, the size at which larvae typically develop into pediveligers. We quantified the delay by first determining the relationship between the proportion of larvae feeding under optimal conditions and time since fertilization. This relationship was best described by the following 3 parameter logistic equations ($F_{1,11}$ = 675.72, $p < 0.0001$, $R^2 = 0.99$):

$$\%\text{Feeding} = \frac{94.1}{\{1+\exp[-0.74 \times (h-45.1)]\}} \quad (1)$$

where h is the hour post-fertilization. The logistic equation was then rearranged and linearized, enabling us to estimate the functional age of larvae feeding in each OA treatment, by comparison with the proportion of larvae feeding under normal conditions.

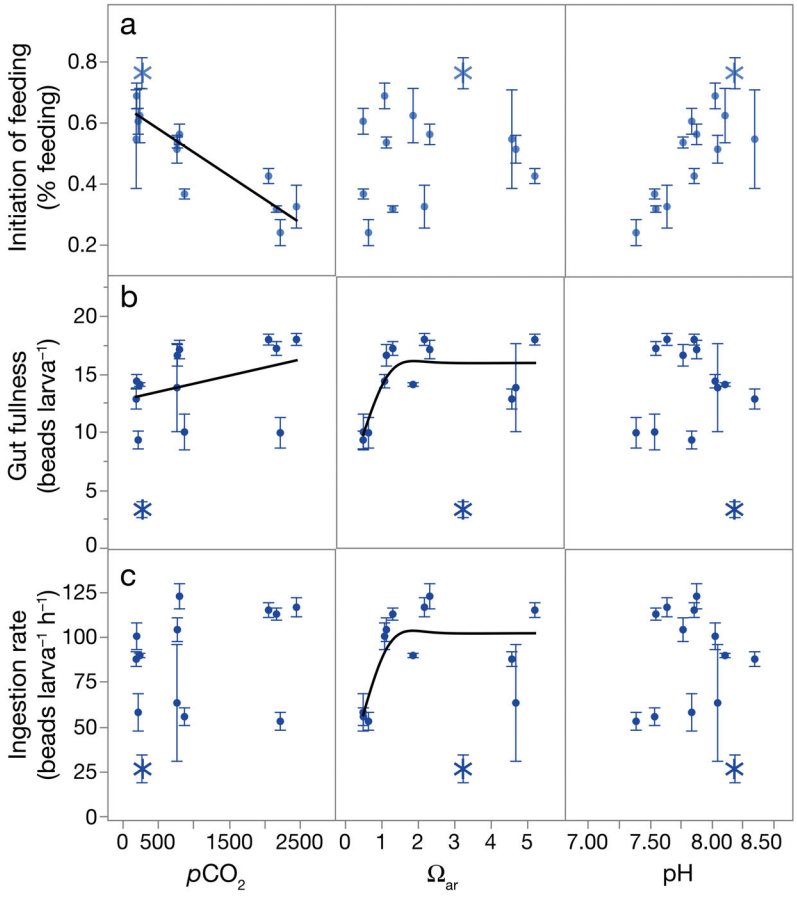

Fig. 1. (a) Proportion of *Mytilus californianus* larvae feeding at 44 h post-fertilization (initiation of feeding), (b) larval gut fullness at 48 h, and (c) larval ingestion rates at 48 h over treatment carbonate chemistries. pCO_2 is in µatm, and pH is expressed in the total scale. Significant relationships between physiological parameters and carbonate chemistry parameters are shown by linear and non-linear functions (lines). Larval ingestion rate and gut fullness from control treatments (Control 2 shown by asterisks in b and c) were identified as outliers and were not included in analyses. Larvae from control treatments in initiation of feeding studies (Control 1 shown by asterisks in a) were included in analyses. Error bars: ±1 SD

Particle processing

To assess the effects of OA on particle processing, 48 h old larvae from each treatment were stocked in nine 25 ml VOA vials (10 larvae ml^{-1}) containing the same water treatment in which they developed from fertilized eggs. After an acclimation period of 1 h, larvae were then exposed to 2 µm Fluoresbrite® Polychromatic (Polysciences) yellow (Y) beads (excitation maxima of 441 nm and emission maxima at 485 nm) at a concentration of 20 beads µl^{-1} and allowed to feed on these beads for 1 h. A second and equal dose of 2 µm red (R) beads (excitation maxima of 491 nm and 512 nm and emission maxima at 554 nm) were added to the vials at a concentration of 20 beads µl^{-1} following the hour-long exposure to Y beads. Triplicate vials were assigned to 1 of 3 exposure groups (10, 30, or 50 min) after R beads were added to the vials. To terminate feeding activity at the prescribed exposure time and preserve larvae for later analysis, 40 µl (0.2% v/v) of 10% buffered formalin (pH: 8.1 to 8.2) were added to the vials. Later, larvae were crushed under a cover slip to flatten gut contents and allow better enumeration of all ingested beads in larvae under an epifluorescent microscope (objective 20×; Leica DM 1000). Larval sample

sizes consisted of ≥20 larvae per replicate vial per treatment.

Gut fullness and ingestion rates

Gut fullness was defined as the mean total number of ingested beads (Y + R beads) per larva over 10, 30, and 50 min sampling periods.

Ingestion rates were estimated by determining the uptake of R beads after the first 10 min of exposure to this bead type. We then doubled the number of ingested beads, as larvae were found to consume R and Y beads at equal rates in preliminary experiments.

Standardizing particle processing for shell-length effects

We examined the relationship between larval shell length (SL), gut fullness, and ingestion rate from a subset of treatments spanning the range of experimental Ω_{ar} categories (≥10 larvae from 10 different VOA vials). Shell lengths, defined as the longest axis parallel to the shell hinge, were obtained by photographing larvae under a light microscope (50×) and measured using Image-Pro v.7.

After finding a significant relationship between larval shell size and feeding metrics (see 'Results'), we applied the following hyperbolic function from Waldbusser et al. (2015b), which strongly predicted the shell lengths of these larvae from the Ω_{ar} (adj. R^2 = 0.88) for the first 48 h of development, to estimate shell lengths of larvae for all treatments:

$$SL = \frac{884.378 \times \Omega_{ar}}{1 + 7.691 \times \Omega_{ar}} \quad (2)$$

Next, we divided gut fullness values and ingestion rates of each treatment by their shell length estimate using Eq. (2). We then reexamined the effects of carbonate chemistry parameters on these feeding metrics after accounting for shell length.

Modeled effects of initial 48 h OA exposure on subsequent larval energy budgets, growth, and development

To estimate the effects of exposure to OA treatments during the first 48 h of larval development on subsequent energy budgets of *M. californianus* larvae, we first estimated energy contents of larvae in treatments at 44 h post-fertilization by applying the relationship between estimated total body energy content (E_{SL}; µJ) and larval shell size reported for *Mytilus edulis* larvae by Sprung (1984a):

$$E_{SL} = 2.28 \times 10^{-7} \times SL^{3.12} \quad (3)$$

where SL is the shell length (µm). To our knowledge, this is the only known allometric relationship between energy content and shell length for any larval *Mytilus* species. Additionally, the relationship provided by Sprung (1984a) seemed appropriate to use here as *M. edulis* and *M. californianus* are similar with respect to egg size and, presumably, energy content (Strathmann 1987).

The total energy contents of larvae (E_T) at 48 h post-fertilization (i.e. after a 4 h period during which larvae could be feeding on algal cells) were then estimated to evaluate the energy budgets of larvae among OA treatments. E_T was estimated by accounting for E_{SL} and other potential energy gains and losses using the following equation:

$$E_T = E_{SL} + \left(\frac{I \times AE}{h} \times (4 - D) \right) - R \quad (4)$$

where I is the ingestion rate (µJ h^{-1}), AE is the assimilation efficiency (%) that describes the conversion of ingested food to energy available to larvae, R is the energy loss due to respiration (µJ) over the 4 h period, and D is the energy gain or loss (µJ) to E_T as a result of developmental advancement or delay in feeding activity. Physiological rate processes were converted to energy units under the following assumptions: (1) growth or change in E_{SL} was negligible between initiation of feeding experiments (44 h) and when the sizes of larvae were measured at 48 h; (2) larval ingestion rates were constant over the period from 44 to 48 h and were equivalent to algal ingestion rates with an estimated algal cell energetic content of 0.61 µJ $cell^{-1}$ (*Isochrysis galbana*; Sprung 1984a), which was also the food source underpinning the relationship between energy content and shell length (Eq. 3); (3) total time for potential gains from ingestion was 4 h ± any advancement or delay in the initiation of feeding among early larvae; (4) assimilation efficiencies of larvae were 0.38 (Sprung 1982); (5) respiration rates were similar among larvae in all treatments except for those of larvae in the lowest pH treatment (based on Waldbusser et al. 2015b); and (6) 1 nl O_2 was equivalent to 20.1 µJ of respired energy (Crisp 1971).

To estimate the impacts of OA during the first 48 h of development on subsequent larval growth, we modeled the developmental time larvae took to reach a shell length of 260 µm, the approximate size of

pediveliger mussel larvae under normal conditions (Sprung 1984a) and a proxy for larval competency for settlement and metamorphosis; however, we note that larval competency is frequently correlated with but not necessarily dependent on larval size (Coon et al. 1990, Pechenik et al. 1996). To make these extrapolations, we first estimated energy content gains of larvae in 24 h intervals (ΔE) using the following equation:

$$\Delta E = E_{SL} + (I \times AE \times NGE) \quad (5)$$

where E_{SL} is the estimated energy content of the larvae based on their shell length at 48 h post-fertilization, I is the ingestion rate (µJ h^{-1}), AE is the assimilation efficiency (%), and NGE is the net growth efficiency (%). E_{SL} and I in this study were assumed constant between 48 and 72 h post-fertilization. After this initial 24 h period (i.e. 48 to 72 h post-fertilization), modeled gains in larval energy content were added to those of larvae of each treatment, and larval shell lengths were adjusted by rearranging Eq. (2). From 72 h post-fertilization onward, we modified larval ingestion rates and larval respiration rates in accordance with allometric equations for *M. edulis* as described by Sprung (1984b,c). This model explicitly tests how an acute initial 48 h OA exposure could significantly alter the subsequent duration and energy budgets of mussel larvae. Assimilation efficiencies were 0.38, 0.29, and 0.27 for larvae <200, between 200 and 250, and >250 µm, respectively (Bayne 1983). NGE were also adjusted for changes in larval size and estimated at 0.78, 0.67, and 0.65 for larvae <200, between 200 and 250, and >250 µm (Bayne 1983). The impacts of differences in initiation of feeding, initial feeding rates, and shell size after 48 h of development on subsequent larval growth to 260 µm were estimated by non-linear multiple regression analysis.

Data analysis

Our experimental seawater treatment design was a 4 × 4 factorial with Ω_{ar} and pCO_2 as the primary factors, with 4 treatment levels of each and 3 replicates treatment^{-1}. Replicates in our experiments represented operator but not biological replicates as they allowed determination of measurement error for the various response metrics but not variation due to biological factors resulting, for example, from genetic differences among mussel populations. Our initial data analysis for all measured responses was a 2-way ANOVA followed by regression analyses to examine linear and non-linear relationships among carbonate chemistry parameters, including possible pH effects within treatment levels of the primary factors. Models for linear and nonlinear regression were selected based upon Akaike's information criterion (Akaike 1973). Assumptions of normality and heteroscedasticity were checked by inspection of data and Shapiro-Wilk's test, and Levene's test, respectively. Initial data analysis found unequal variance across treatment groups and replicates in the proportion of mussel larvae feeding; therefore, treatment means were used to reduce heteroscedasticity. In particle processing experiments, larvae from all the control treatment replicates (Control 2 larvae: unaltered, filtered seawater reared in open 10 l polyethylene aquaria) fed on R beads at unusually low rates and were identified as outliers from residual plots and leverage tests when we examined their ingestion rate and gut fullness values. These larvae we likely either mishandled or improperly exposed to R beads during this portion of our study; although we left the points in the figures, data from these control treatments were removed prior to both gut fullness and ingestion rate analyses. Larvae across all 'MedLow' pCO_2 treatments also had unusually low ingestion rates. We attributed this to human error due to either bead stocking error or improper handling of vials after introducing beads; therefore, we removed data from these samples prior to regressing ingestion rate data against carbonate chemistry and gut fullness data. For their inclusion in other modeling efforts (scope for growth, SfG; growth, etc.), ingestion rates of larvae from MedLow pCO_2 treatments were estimated from the Ω_{ar} and applying Eq. (6). All statistical analyses were conducted using JMP v.12 (SAS Institute).

RESULTS

Chemistry manipulations

Although there was some variability in carbonate chemistry parameters within treatment levels, the variability was generally far less than the differences among treatments. Two treatments deviated from targets: Low Ω_{ar} / MedLow pCO_2, and MedHigh Ω_{ar} / Low pCO_2. In the former, a preservation issue appeared to have caused pCO_2 to be 3× higher than expected with a concomitant decrease in Ω_{ar}. In the latter deviation, we suspected precipitation to be the cause of unexpected low alkalinity (82 µmol kg^{-1}), resulting in the pCO_2 of this treatment to be greater (excess of 41 µatm) than for other low pCO_2 treatments.

Delay of initiation of feeding

After rearranging and linearizing Eq. (1), we regressed larval age estimates against their respective pCO_2 values and found a significant predictive linear relationship ($F_{1,14} = 34.55$, $p < 0.0001$, $R^2 = 0.70$). From this analysis, we estimated a 5 min functional delay in initiation of feeding for every 100 µatm increase in pCO_2 in treatment seawater, relative to the functional age of larvae reared under optimal conditions (Fig. 2, Table 2).

Particle processing

Gut fullness

Gut fullness varied significantly among treatments due to Ω_{ar} ($F_{3,32} = 17.51$, $p < 0.0001$) and pCO_2 ($F_{3,32} = 11.30$, $p < 0.0001$) with a significant interaction term ($F_{9,32} = 3.06$, $p = 0.0093$; Fig. 1b, Table 2). A 3-parameter logistic equation similar to Eq. (1) best described how gut fullness varied as a function of Ω_{ar} ($F_{1,14} = 13.37$, $p = 0.0026$, $R^2 = 0.48$). Gut fullness was also found to weakly, yet significantly, respond positively to increasing pCO_2 ($F_{1,14} = 4.73$, $p = 0.0472$, $R^2 = 0.25$) (Fig. 1b). Gut fullness was not predicted by pH ($F_{1,15} = 0.09$, $p = 0.7608$).

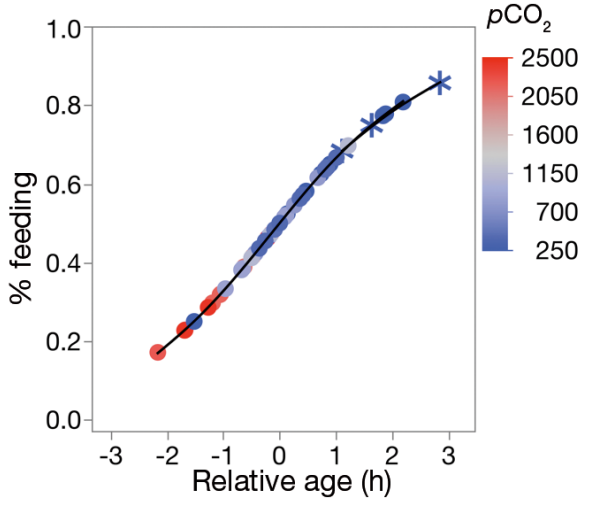

Fig. 2. Relative functional age of *Mytilus californianus* larvae for pCO_2 treatments were estimated based on the proportion of larvae feeding at 44 h in each treatment and are relative to larvae in preliminary studies in which 50% of larvae were observed to be feeding at 44 h post-fertilization under optimal conditions (~380 ppm pCO_2 and 18°C). The relationship between % feeding over time as larvae develop can be found in Table 2. Colored circles represent actual pCO_2 values in treatments (µatm) with their actual % feeding values superimposed on the age function. Asterisks: Control 1 treatments

Table 2. Linear and non-linear effects of seawater carbonate chemistry on initiation of *Mytilus californianus* larval feeding (% larvae feeding at 44 h post-fertilization), relative age (hours), gut fullness (GF; beads $larva^{-1}$), and ingestion rate (IR; beads $larva^{-1}$ h^{-1}). Standard errors for parameter estimates are given in parentheses. 'Relative functional age' of larvae is expressed as relative to the age of larvae when 50% were found to feed under normal conditions (44 h)

Metric	Effect	Model	Parameter estimates	df	*F*	p	R^2
Initiation of feeding	pCO_2	% Feeding = $a + b\,pCO_2$	$a = 0.84$ (0.03), $b = -0.0001$ (0.00000)	1,14	43.73	<0.0001	0.73
Relative functional age	pCO_2	Age = $a + b\,pCO_2$	$a = 46.33$ (0.16), $b = -0.0008$ (0.0001)	1,14	42.42	<0.0001	0.75
Gut fullness	Ω_{ar}	GF = $c / \{1 + e^{[-a(\Omega_{ar} - b)]}\}$	$a = 2.32$ (1.47), $b = 0.08$ (0.28), $c = 16.59$ (0.84)	1,14	13.37	0.0026	0.49
Gut fullness	pCO_2	GF = $a + b\,pCO_2$	$a = 13.42$ (0.99), $b = 0.002$ (8.1×10^{-4})	1,14	4.73	0.0472	0.25
Gut fullness	$\Omega_{ar} \times pCO_2$	GF = $a + b\,pCO_2$ by Ω_{ar}	See Table S1 in the Supplement for intercept estimates	4,15	8.52	0.0022	0.75
Ingestion rate	Ω_{ar}	IR = $a + be^{(c \times \Omega_{ar})}$	$a = 102.03$ (5.62), $b = -278.79$ (333), $c = -3.43$ (2.34)	1,11	12.58	0.0053	0.56
Ingestion rate	Shell length	IR = $a + b$SL	$a = -137.38$ (87.6), $b = 2.18$ (0.84)	1,11	6.76	0.0256	0.40
Gut fullness	Ingestion rate	GF = $a + b$IR	$a = 3.79$ (1.63), $b = 0.11$ (0.01)	1,11	43.89	<0.0001	0.81

To explore the interaction between Ω_{ar} and pCO_2 on gut fullness, we constructed a multiple linear regression with pCO_2 among Ω_{ar} treatment categories (see Fig. S1 in the Supplement at www.int-res.com/articles/suppl/m563p081_supp.pdf). In a full multiple linear regression model (factors: Ω_{ar}, pCO_2, and $\Omega_{ar} \times pCO_2$), slope estimates of regressed Ω_{ar} categories were found to be similar ($F_{7,15} = 4.92$, $pCO_2 \times \Omega_{ar}$ p = 0.538). Under a reduced multiple linear regression model (factors: Ω_{ar} and pCO_2), pCO_2 was still a significant predictor of gut fullness ($F_{3,15} = 13.31$, p = 0.0038), and significant differences were observed between the intercepts of some Ω_{ar} treatments ($F_{3,15} = 7.57$, Ω_{ar} category p = 0.0051). Larvae from the low Ω_{ar} category had significantly lower gut fullness values as a function of pCO_2 relative to all other Ω_{ar} categories (Tukey's HSD, $\alpha = 0.05$).

Ingestion rates

Using a 2-way ANOVA, larval ingestion rates were not found to vary significantly with pCO_2 ($F_{2,24} = 2.28$, p = 0.1239), but were significantly predicted by Ω_{ar} ($F_{3,24} = 15.22$, p < 0.0001; Fig. 1c). The interaction term between pCO_2 and Ω_{ar} was not found to be a significant predictor of ingestion rates ($F_{6,24} = 2.08$, p = 0.0925). We regressed ingestion rates against Ω_{ar} ($F_{1,11} = 12.58$, p = 0.0053, $R^2 = 0.56$; Fig. 1c) and this relationship was best described by the following 3-parameter exponential model:

$$\text{Ingestion} = a + b\text{Exp}^{(c \times \Omega_{ar})} \quad (6)$$

where a is the asymptote, b is the scale, and c is the curve's growth rate (see Table 2 for parameter estimates). A significant and positive relationship was found between ingestion rates and gut fullness measured across the entire spectrum of Ω_{ar} treatments ($F_{1,11} = 43.89$, p < 0.0001, $R^2 = 0.81$; Fig. 3c).

Standardizing gut fullness and ingestion rate for differences in shell lengths

The relationship between Ω_{ar} and shell lengths examined among a subset of data was similar to that found by Waldbusser et al. (2015b) for all larvae across all treatments (Fig. 3a). Furthermore, we found ingestion rates were positively correlated with larval shell lengths ($F_{1,11} = 6.76$, p = 0.0265, $R^2 = 0.40$; Fig. 3b) among the subset of treatments examined. After standardizing physiological processes by shell lengths, Ω_{ar} was found to no longer be a significant predictor of gut fullness ($F_{1,15} = 4.02$, p = 0.0644, $R^2 = 0.019$) but still explained 41% of the variation in larval ingestion rates ($F_{1,11} = 7.0007$, p = 0.0245).

Modeled effects of initial 48 h OA exposure on subsequent larval energy budgets, growth, and development

Larval energy content based on shell length (E_{SL}) and total larval energy content (E_T) for 48 h old larvae were both strongly correlated with Ω_{ar} (E_{SL}: $F_{1,16} = 235.76$, p < 0.0001, $R^2 = 0.94$; E_T: $F_{1,16} = 268.29$, p < 0.0001, $R^2 = 0.94$), while treatment pCO_2 and pH were not significant predictors of E_{SL} or E_T (p > 0.05). E_{SL} ranged from 304 to 708 µJ larva^{-1} (see Table S3 in the Supplement) and was a function of Ω_{ar} (Fig. 4a, Table S2). After adding the potential gains from in-

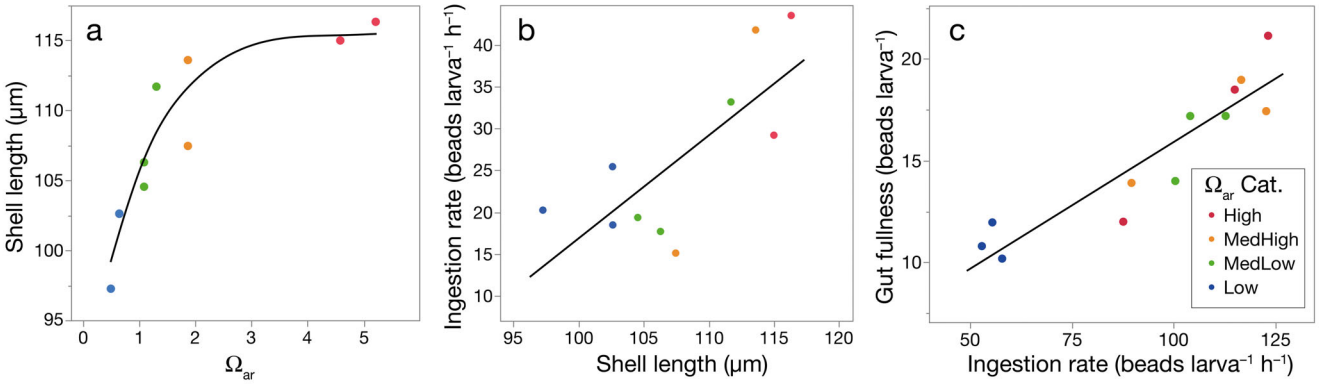

Fig. 3. Relationships between experimental conditions and morphological and physiological metrics: (a) *Mytilus californianus* shell length versus aragonite saturation state (dots are from this study and are fitted to Eq. 2 derived from Waldbusser et al. 2015b), (b) ingestion rate versus shell length, and (c) gut fullness versus ingestion rate. For (a) and (b), dots represent single replicate means within treatments from the subset of data analyzed for the effect of shell size (see 'Materials and methods; Standardizing particle processing for shell-length effects'), while dots in (c) represent treatment means. Values for each 'Ω_{ar} Cat.' can be found in Table 1

gestion and subtracting expenditures of respiration and delay in the initiation of feeding, E_T at 48 h post-fertilization ranged from 336 to 790 µJ larva^{-1}. By subtracting E_T from E_{SL}, we arrived at an estimate of SfG, as this was the energy gained or lost during the 4 h period between 44 and 48 h (Fig. 4b). We estimated that SfG ranged from −6.72 to 82.9 µJ larva^{-1} (Table S3); the only larvae estimated to have negative SfG were those from treatment Low Ω_{ar} / MedLow pCO_2, which were previously measured by Waldbusser et al. (2015b) as having elevated respiration rates. On average, SfG was significantly lower (mean 27.19 µJ larva^{-1}) for larvae incubated in undersaturated Ω_{ar} conditions (t_{15} = 4.68, p < 0.0179). Conversely, larvae in supersaturated Ω_{ar} treatments had a much greater surplus of energy (mean: 80.71 µJ larva^{-1}) that was available for growth (Table S3).

Non-linear regression analysis was used to model shell growth of *Mytilus californianus* larvae over time to the pediveliger stage by Ω_{ar} category because Ω_{ar} alone predicted larval shell length (see Eq. 2) and, consequently, larval energy content (Eq. 3). Estimated development time to the pediveliger stage (260 µm) was 22.6, 18.5, 18.0, and 17.6 d for Low, MedLow, MedHigh, and High Ω_{ar} categories, respectively (Fig. 5, Table 3). Larvae from undersaturated Ω_{ar} treatments were predicted to grow at a significantly slower rate than those in supersaturated conditions ($\Omega_{ar} \geq 1$; analysis of means [ANOM], $\alpha = 0.05$).

We modeled the potential effects of differences in larval size, initiation of feeding, and ingestion rates due to Ω_{ar} treatments during the first 48 h of development on subsequent development time to the pediveliger stage. To separate the effects of initiation of feeding, we started by removing the energetic impacts of delay of feeding so that larvae from all OA treatments were modeled to begin feeding at exactly 44 h of development. We then compared the time for larvae to grow to 260 µm under each Ω_{ar} treatment and control. To estimate the impacts of OA on ingestion rates, shell size, and respiration on larval development time, we first applied the average values for each metric (15 beads larva^{-1} h^{-1}, 104 µm, 0.15 nl O_2 larva^{-1} h^{-1}, respectively) across treatments for the first 48 h of development. These average physiological rates were close to values found for larvae at Ω_{ar} = 1. We then modeled development times for larvae to reach 260 µm and subtracted development times from full models containing all impacts. Therefore, we report on the hours gained or lost by larvae as a result of OA impacts relative to larvae held at $\Omega_{ar} \approx 1$. We used 95% confidence intervals for estimates of

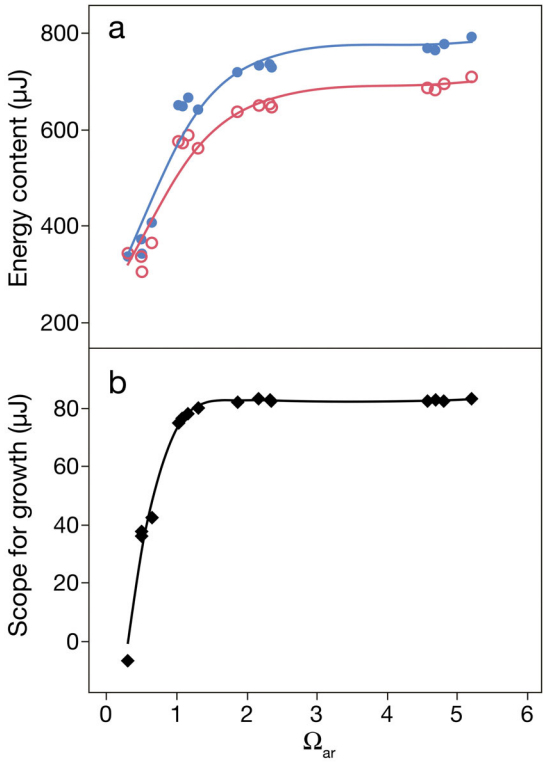

Fig. 4. (a) Estimated *Mytilus californianus* larval energy content based on shell size (E_{SL}; open circles), total energy content (E_T; closed circles) and (b) scope for growth (diamonds) of 48 h old (post-fertilization) *M. californianus* larvae plotted against aragonite saturation state (Ω_{ar}) (see Eq. 4). Data points: treatment means

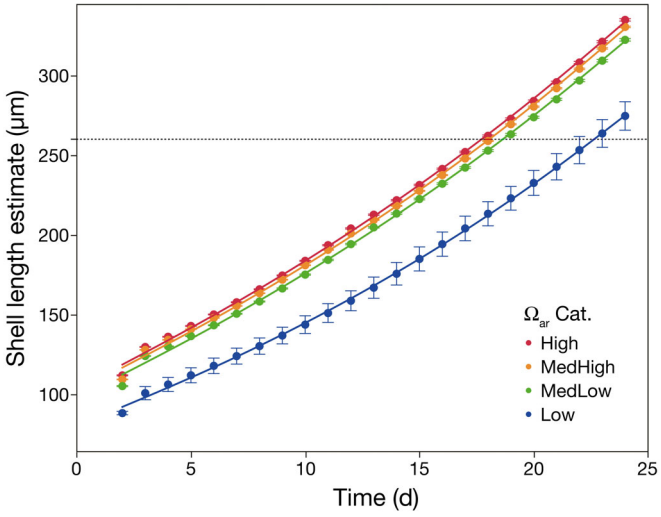

Fig. 5. Modeled shell growth of *Mytilus californianus* larvae over time after exposure to various aragonite saturation state categories (Ω_{ar} Cat.; see Table 1 for values) during the first 48 h of development. Intersections of the colored lines and the dashed horizontal line indicate the estimated ages of *Mytilus* larvae reaching the pediveliger stage (260 µm). Error bars: SD

Table 3. Modeled development times of *Mytilus californianus* larvae to reach the pediveliger stage (260 µm) across aragonite saturation state categories (Ω_{ar} Cat.; see Table 1 for values). Factors influencing developmental time among Ω_{ar} categories are initiation of feeding (IF; % larvae feeding) at 44 h post-fertilization, and ingestion rates (beads larva^{-1} h^{-1}), and shell length (µm) at 48 h. Developmental time advancement (negative values) or delay (positive values) are expressed in hours with significant impacts denoted by asterisks (*). Upper and lower 95% confidence intervals (CI) are for development times to the pediveliger stage. Delay and advancement of developmental times are relative to larvae held at approximately Ω_{ar} = 1 and under similar Ω_{ar} conditions to category 'MedLow'

Ω_{ar} Cat.	Mean % IF among 44 h old larvae (% feeding)	Mean ingestion rates among 48 h old larvae (beads larva^{-1} h^{-1})	Mean shell length among 48 h old larvae (µm)	Development time to pediveliger stage (d)	Lower 95% CI	Upper 95% CI	IF delay effect (h)	Ingestion rates effect (h)	Shell length effect (h)
High	0.56	17.74	111.68	17.72	17.66	17.77	0.00	7.21*	20.84*
MedHigh	0.56	17.66	109.14	18.06	18.01	18.11	0.00	1.94	12.87*
MedLow	0.55	16.34	104.94	18.65	18.59	18.70	0.00	3.64*	4.35*
Low	0.55	7.82	87.99	22.65	22.25	23.05	0.00	−53.60*	−54.19*

development time to determine the significance of factors that might impact development (Table 3).

The energetic effects of pCO_2 on the initiation of feeding (range: −0.08 to 0.04 µJ larva^{-1}) were not significant in delaying the modeled larvae growth. Conversely, Ω_{ar} impacts on initial shell length and ingestion rates during the first 48 h of development were significant factors in determining subsequent larval developmental times among many of the Ω_{ar} categories; however, the intensity of their impacts varied by Ω_{ar} category (Table 3). The effect of Ω_{ar} on initial shell length advanced or delayed larval development to 260 µm by −54.19 and 20.84 h, respectively. Ω_{ar} effects on larval ingestion rates resulted in −53.60 to 7.21 h in developmental advancement or delay, respectively.

DISCUSSION

Mechanistic understanding of OA impacts on larval feeding physiology

Initiation of feeding, gut fullness, and ingestion rates of *Mytilus californianus* larvae all varied in response to OA but were not necessarily driven by a common carbonate chemistry parameter. In Waldbusser et al. (2015b), we found the initiation of feeding among *M. californianus* was primarily correlated with pCO_2 (Fig. 1a) and suggested that CO_2 might have been impacting feeding organ functionality (i.e. velum cilia beat frequency) (Schmid et al. 2007) or possibly disrupting nerve synapse performance (Peracchia 2004). Upon incorporation of additional data and reanalysis, we determined CO_2 created a 5 min functional age delay in initiation of feeding for every increase of 100 µatm pCO_2 in ambient seawater (Fig. 2) and that eventually almost all larvae (>90%) began to feed in our studies. Reduced developmental rates and delayed onset of critical behaviors occurred among other invertebrate species when held in high pCO_2 environments (Kurihara et al. 2004, Mayor et al. 2007, Ellis et al. 2009), but it remains poorly understood how elevated concentrations of this carbonate species impact larval development and physiological processes.

Gut fullness is rarely measured in larval feeding studies, but it provides insights into relationships between particle processing behaviors (Penry 2000, Gray et al. 2015). pCO_2 was found to be weakly and positively correlated with gut fullness (R^2 = 0.25). In addition, gut fullness was positively correlated with Ω_{ar}, with a 49% change in gut fullness across the tested range of Ω_{ar} treatments (Fig. 1b); however, further analysis indicated that Ω_{ar} impacted gut fullness as a result of its positive correlation with shell size. High pCO_2 values may have slowed bead passage through the gut lumen, resulting in bead accumulation. Internal organs and digestive mechanisms involved in particle processing (e.g. cilia activity, peristalsis and crystalline style rotation) may be sensitive to pCO_2, especially if intracellular pH is not maintained due to changes in CO_2 diffusion rates across cellular membranes caused by elevated extracellular pCO_2 conditions (Vandenberg et al. 1994).

Ω_{ar} effects on larval ingestion rates were, in part, due to a positive correlation with larval shell length (Figs. 1c & 3a,b); however, Ω_{ar} also had a substantial independent effect on ingestion rates (41 of the 56% of explained variance) after accounting for shell length effects. Shells form structures for the attachment of feeding organs and could play a key role in their functioning (Simkiss & Wilbur 1989); for example, poor attachment of velar retractor muscles to the

interior of the larval shell may affect velar movement and particle processing efficiencies. Additionally, shell abnormalities, which were more evident under low Ω_{ar} conditions (Waldbusser et al. 2015b), may affect hinge structure and shell movements associated with velar swimming and feeding (Talmage & Gobler 2010). Several studies have indicated the importance of food supply in meeting increased energetic demands of calcification under OA conditions (Melzner et al. 2011, Pansch et al. 2014, Ramajo et al. 2016). Reductions in larval ingestion rates due to the effects of low Ω_{ar} conditions will have a negative effect on rates of energy acquisition and reduce the capacity of larvae to meet increased energetic demands due to OA conditions.

Modeled effects of carbonate chemistry parameters on larval energy budgets and growth

Energetically, the impacts of delays in initiation of feeding were minor (range: −0.08 to 0.04 µJ larva^{-1}) and orders of magnitude lower than those of other impacted energy budget components estimated in this study (see Table S3 in the Supplement at www.int-res.com/articles/suppl/m563p081_supp.pdf). Additionally, when this delay was incorporated into larval growth models, it was found to have a negligible effect on subsequent growth (Table 3), suggesting that not all measured OA physiological impacts on larvae have significant long-term effects on animal fitness.

Estimates of larval energy content based on shell length (i.e. E_{SL}) varied significantly among experimental treatments (range: 304 to 708 µJ larva^{-1}) and provided a coarse measure of the energetic impact of OA on development from the fertilized egg to the shelled stage. Across Ω_{ar} treatments, larvae from $\Omega_{ar} < 1$ treatments had half the estimated energy content of larvae in $\Omega_{ar} \geq 1$ treatments (Fig. 4a). Accounting for metabolic energy gains and losses (E_T) from ingestion and respiration (measured in Waldbusser et al. 2015b) accentuated these differences in larval energy content (Fig. 4a).

SfG across the range of Ω_{ar} was estimated from differences between energy gains and losses (i.e. ingestion−respiration). Differences in SfG estimates were largely driven by varying ingestion rates across Ω_{ar} treatments. SfG values indicated that larvae in $\Omega_{ar} \geq 1$ seawater treatments would have acquired energy (i.e. 74 to 82 µJ in 4 h) while larvae from $\Omega_{ar} < 1$ seawater treatments, which had much lower ingestion rates, acquired less energy (SfG range: −6.72 to 42 µJ; Fig. 4b & Table S3). The negative SfG value for Low Ω_{ar} / MedLow larvae was due to their greater respiration rates (measured in Waldbusser et al. 2015b) in combination with low ingestion rates, indicating these larvae were still likely be reliant on maternal energy stores to fuel metabolism. To put our SfG values into a development context, Waldbusser et al. (2013) estimated an energetic cost of ~24 µJ for *Crassostrea gigas* larvae to synthesize their first layer of shell. SfG values in combination with Ω_{ar}-dependent size data from Waldbusser et al. (2015b) agrees well with other observations that larvae held in $\Omega_{ar} < 1$ conditions must allocate more energy towards other developmental processes at the expense of shell growth and/or are less efficient at growing shell due to the energetic constraints of shell synthesis (Kurihara 2008, Gaylord et al. 2011, Waldbusser et al. 2013).

We were able to model larval development over time by utilizing established allometric relationships between *Mytilus* larval shell length, energy content, and ingestion rates. We estimated the average time for larvae, initially exposed to $\Omega_{ar} \geq 1$ conditions for 48 h, to reach the pediveliger stage (260 µm) to be approximately 18 d post-fertilization i.e. within the reported range of 9 to 35 d for the larval stage of *M. californianus* (Bayne et al. 1976, Strathmann 1987, Seed & Suchanek 1992, Gaylord et al. 2011). After accounting for the physiological impacts of OA on *M. californianus* during the first 48 h of larval development, we estimated that larvae from $\Omega_{ar} < 1$ treatments would subsequently incur a developmental delay of 4.9 d in reaching the pediveliger stage, compared with larvae initially exposed to supersaturated conditions ($\Omega_{ar} \gg 1$; Fig. 5) i.e. a 27% increase in the duration of the larval stage.

Larval developmental delays due to OA stress have been reported previously for bivalves (Kurihara et al. 2007, Talmage & Gobler 2009, Gazeau et al. 2010, Gaylord et al. 2011, Timmins-Schiffman et al. 2013), urchins (Dupont & Thorndyke 2008, Stumpp et al. 2011), krill (Kawaguchi et al. 2013), crabs (Walther et al. 2010), and other taxa. Delays in metamorphosis may have significant ecological implications. A prolonged planktonic stage may reduce survival as it increases exposure time to predators (Rumrill 1990) and other stresses such as ultraviolet radiation (Peachey 2005). Greater time spent in the pelagic zone also increases the potential for larval advection away from favorable habitats (Strathmann 1985). Furthermore, delaying the arrival time of pediveliger larvae may put *M. californianus* at a competitive disadvantage compared with earlier settling species, if available settlement substrate is limiting (Kennedy 1996).

There are several assumptions and limitations in our approach in estimating E_{SL}, SfG, E_T, and development of larvae by our model. First, we estimated larval energy content at 44 h (i.e. E_{SL}) based on the relationship between ash free dry tissue weight (AFDW) and larval shell length reported by Sprung (1984a). This relationship did not account for possible differences in the ratios of shell size and tissue weights that can occur in *M. californianus* larvae under OA stress (Gaylord et al. 2011). Second, the model did not account for possible differences in growth efficiencies of larvae in OA treatments that have been observed with *M. californianus* larvae (Gaylord et al. 2011). For instance, we assumed similar digestive and assimilation efficiencies across treatments; however, other investigators have found that digestive efficiencies and digestive rates of larval urchins are impacted by OA (Stumpp et al. 2013). Third, we did not allow for any compensatory growth of OA-impacted modeled larvae, yet we acknowledge this may be important in the recovery of nutritionally-stressed bivalve larvae and other marine invertebrates (Moran & Manahan 2004, Yan et al. 2009). Given these assumptions and uncertainties surrounding our model, further studies should be conducted to directly measure OA impacts on larval physiological and energetic processes that could affect development.

In summary, OA impacts on the feeding physiology of bivalve larvae may limit their ability to efficiently acquire energy. This finding is supported by studies that have shown that OA can affect various feeding physiological and metabolic processes, including particle selection (Vargas et al. 2013), ingestion (Vargas et al. 2015), gut fullness (this study), digestion (Stumpp et al. 2013), and SfG (Stumpp et al. 2011) in marine invertebrate larvae. We identified pCO_2 and Ω_{ar} as 2 carbonate chemistry parameters that affected larval feeding responses. Our model suggested that acute OA impacts on larval development and feeding physiology during the first 48 h of development could delay subsequent growth to the pediveliger stage.

Acknowledgements. The authors thank Thaddaeus Buser for helping count beads and Javan Bailey and Greg Hutchinson of the Molluscan Broodstock Program, Oregon State University, for supplying technical and infrastructural support during studies. Execution of experiments was aided by Greg Hutchinson, Iria Gimenez, Cale Miller, Elizabeth Brunner, and Becky Mabardy. Project funding was primarily provided by National Science Foundation Grant OCE CRI-OA #1041267 awarded to G.G.W., B.H., and C.J.L. Additional support to M.W.G. was provided by the Oregon Society of Conchologists and the Markham Scholarship Fund, Hatfield Marine Science Center. Data from this study are available on the website of the National Science Foundation website, Biological and Chemical Ocean Oceanography Data Management Office (BCO-DMO) (OA Feeding physiology: http://www.bco-dmo.org/dataset/662154; OA Modeled Growth: http://www.bco-dmo.org/dataset/662188) Support to M.W.G. was also provided by National Science Foundation award #11A-1355457 to Maine EPSCoR at the University of Maine.

LITERATURE CITED

Akaike H (1973) Information theory and an extension of the maximum likelihood principle. In: Petrov BN, Csaki F (eds) Proc 2nd Int Symp Information Theory, Tsahkadsor, Armenia. Akademiai Kiado, Budapest, p 267–281

Armengol X, Boronat L, Camacho A, Wurtsbaugh WA (2001) Grazing by a dominant rotifer *Conochilus unicornis* Rousselet in a mountain lake: *in situ* measurements with synthetic micro-spheres. Hydrobiologia 446-447: 107–114

Baldwin BS, Newell RIE (1995) Relative importance of different size food particles in the natural diet of oyster larvae *Crassostrea virginica*. Mar Ecol Prog Ser 120:135–145

Barton A, Hales B, Waldbusser GG, Langdon C, Feely RA (2012) The Pacific oyster, *Crassostrea gigas*, shows negative correlation to naturally elevated carbon dioxide levels: implications for near-term ocean acidification effects. Limnol Oceanogr 57:698–710

Bayne B (1983) Physiological ecology of marine molluscan larvae. In: Wilbur KM (ed) The Mollusca. Academic Press, New York, NY, p 299–343

Bayne BL, Bayne CJ, Carefoot TC, Thompson RJ (1976) The physiological ecology of *Mytilus californianus* Conrad. 1. Metabolism and energy balance. Oecologia 22:211–228

Coon SL, Fitt WK, Bonar DB (1990) Competence and delay of metamorphosis in the Pacific oyster *Crassostrea gigas*. Mar Biol 106:379–387

Crisp DJ (1971) Energy flow measurements. In: Holme NA, McIntyre AD (eds) Methods for the study of marine benthos. Blackwell, Oxford, p 197–279

Dadd RH (1971) Effects of size and concentration of particles on rates of ingestion of latex particulates by mosquito larvae. Ann Entomol Soc Am 64:687–692

DeMott WR (1988) Discrimination between algae and artificial particles by freshwater and marine copepods. Limnol Oceanogr 33:397–408

Dickson AG (1990) Standard potential of the reaction: $AgCl(s) + ½H_2(g) = Ag(s) + HCl(aq)$, and the standard acidity constant of the ion HSO^-_4 in synthetic seawater from 273.15 to 318.15 K. J Chem Thermodyn 22:113–127

Doney SC, Fabry VJ, Feely RA, Kleypas JA (2009) Ocean acidification: the other CO_2 problem. Annu Rev Mar Sci 1:169–192

Dupont S, Thorndyke MC (2008) Ocean acidification and its impact on the early life-history stages of marine animals. In: Briand F (ed) CIESM workshop monographs: impacts of acidification on biological, chemical and physical systems in the Mediterranean and Black Seas. CIESM, Monaco, p 89–97

Ellis RP, Bersey J, Rundle SD, Hall-Spencer JM, Spicer JI (2009) Subtle but significant effects of CO_2 acidified seawater on embryos of the intertidal snail, *Littorina obtusata*. Aquat Biol 5:41–48

Espinosa EP, Perrigault M, Ward JE, Shumway SE, Allam B (2009) Lectins associated with the feeding organs of the oyster *Crassostrea virginica* can mediate particle selection. Biol Bull (Woods Hole) 217:130–141

Feely RA, Sabine CL, Hernandez-Ayon JM, Ianson D, Hales B (2008) Evidence for upwelling of corrosive 'acidified' water onto the continental shelf. Science 320:1490–1492

Gaylord B, Hill TM, Sanford E, Lenz EA and others (2011) Functional impacts of ocean acidification in an ecologically critical foundation species. J Exp Biol 214: 2586–2594

Gazeau F, Gattuso JP, Dawber C, Pronker AE and others (2010) Effect of ocean acidification on the early life stages of the blue mussel (*Mytilus edulis*). Biogeosciences Discuss 7:2051–2060

Gray MW, Kramer S, Langdon C (2015) Particle processing and gut kinematics of planktotrophic bivalve larvae. Mar Biol 162:2187–2201

Hart MW (1991) Particle captures and the method of suspension feeding by echinoderm larvae. Biol Bull 180:12–27

Kawaguchi S, Ishida A, King R, Raymond B and others (2013) Risk maps for Antarctic krill under projected Southern Ocean acidification. Nat Clim Change 3:843–847

Kennedy VS (1996) Biology of larvae and spat. In: Kennedy VS, Newell RIE, Eble AF (eds) The eastern oyster *Crassostrea virginica*. Maryland Sea Grant College Publication, College Park, MD, p 371–421

Kurihara H (2008) Effects of CO_2-driven ocean acidification on the early developmental stages of invertebrates. Mar Ecol Prog Ser 373:275–284

Kurihara H, Shimode S, Shirayama Y (2004) Sub-lethal effects of elevated concentration of CO_2 on planktonic copepods and sea urchins. J Oceanogr 60:743–750

Kurihara H, Kato S, Ishimatsu A (2007) Effects of increased seawater pCO_2 on early development of the oyster *Crassostrea gigas*. Aquat Biol 1:91–98

Kurihara H, Asai T, Kato S, Ishimatsu A (2008) Effects of elevated pCO_2 on early development in the mussel *Mytilus galloprovincialis*. Aquat Biol 4:225–233

Mayor DJ, Matthews C, Cook K, Zuur AF, Hay S (2007) CO_2-induced acidification affects hatching success in *Calanus finmarchicus*. Mar Ecol Prog Ser 350:91–97

Melzner F, Stange P, Trübenbach K, Thomsen J and others (2011) Food supply and seawater pCO_2 impact calcification and internal shell dissolution in the blue mussel *Mytilus edulis*. PLOS ONE 6:e24223

Milke LM, Ward JE (2003) Influence of diet on pre-ingestive particle processing in bivalves: II. Residence time in the pallial cavity and handling time on the labial palps. J Exp Mar Biol Ecol 293:151–172

Millero FJ (1995) Thermodynamics of the carbon dioxide system in the oceans. Geochim Cosmochim Acta 59: 661–677

Millero FJ (2010) Carbonate constants for estuarine waters. Mar Freshw Res 61:139–142

Moran AL, Manahan DT (2004) Physiological recovery from prolonged 'starvation' in larvae of the Pacific oyster *Crassostrea gigas*. J Exp Mar Biol Ecol 306:17–36

Pace ML, Bailiff MD (1987) Evaluation of a fluorescent microsphere technique for measuring grazing rates of phagotrophic microorganisms. Mar Ecol Prog Ser 40:185–193

Pan TCF, Applebaum SL, Manahan DT (2015) Experimental ocean acidification alters the allocation of metabolic energy. Proc Natl Acad Sci USA 112:4696–4701

Pansch C, Schaub I, Havenhand J, Wahl M (2014) Habitat traits and food availability determine the response of marine invertebrates to ocean acidification. Glob Change Biol 20:765–777

Peachey RBJ (2005) The synergism between hydrocarbon pollutants and UV radiation: a potential link between coastal pollution and larval mortality. J Exp Mar Biol Ecol 315:103–114

Pechenik JA, Hammer K, Weise C (1996) The effect of starvation on acquisition of competence and post-metamorphic performance in the marine prosobranch gastropod *Crepidula fornicata* (L.). J Exp Mar Biol Ecol 199:137–152

Penry DL (2000) Digestive kinematics of suspension-feeding bivalves: modeling and measuring particle-processing in the gut of *Potamocorbula amurensis*. Mar Ecol Prog Ser 197:181–192

Peracchia C (2004) Chemical gating of gap junction channels: roles of calcium, pH and calmodulin. Biochim Biophys Acta BBA Biomembr 1662:61–80

Ramajo L, Pérez-León E, Hendriks IE, Marbà N and others (2016) Food supply confers calcifiers resistance to ocean acidification. Sci Rep 6:19374

Rumrill SS (1990) Natural mortality of marine invertebrate larvae. Ophelia 32:163–198

Schmid A, Sutto Z, Nlend MC, Horvath G and others (2007) Soluble adenylyl cyclase is localized to cilia and contributes to ciliary beat frequency regulation via production of cAMP. J Gen Physiol 130:99–109

Seed R, Suchanek TH (1992) Population and community ecology of *Mytilus*. In: Gosling E (ed) The mussel *Mytilus*: ecology, physiology, genetics and culture. Elsevier Science Publishers, Amsterdam, p 87–169

Simkiss K, Wilbur KM (1989) Biomineralization: cell biology and mineral deposition. Academic Press, San Diego, CA

Solow AR, Gallager SM (1990) Analysis of capture efficiency in suspension feeding: application of nonparametric binary regression. Mar Biol 107:341–344

Sprung M (1982) Untersuchungen zum Energiebudget der Larven der Miesmuschel, *Mytilus edulis*. PhD thesis, University of Kiel

Sprung M (1984a) Physiological energetics of mussel larvae (*Mytilus edulis*). I. Shell growth and biomass. Mar Ecol Prog Ser 17:283–293

Sprung M (1984b) Physiological energetics of mussel larvae (*Mytilus edulis*). II. Food uptake. Mar Ecol Prog Ser 17: 295–305

Sprung M (1984c) Physiological energetics of mussel larvae (*Mytilus edulis*). III. Respiration. Mar Ecol Prog Ser 18: 171–178

Strathmann RR (1985) Feeding and nonfeeding larval development and life-history evolution in marine invertebrates. Annu Rev Ecol Syst 16:339–361

Strathmann MF (1987) Reproduction and development of marine invertebrates of the northern Pacific coast: data and methods for the study of eggs, embryos, and larvae. University of Washington Press, Seattle, WA

Stumpp M, Wren J, Melzner F, Thorndyke MC, Dupont ST (2011) CO_2 induced seawater acidification impacts sea urchin larval development I: Elevated metabolic rates decrease scope for growth and induce developmental delay. Comp Biochem Physiol A Mol Integr Physiol 160: 331–340

Stumpp M, Hu M, Casties I, Saborowski R, Bleich M, Melzner F, Dupont S (2013) Digestion in sea urchin larvae impaired under ocean acidification. Nat Clim Change 3:1044–1049

Talmage SC, Gobler CJ (2009) The effects of elevated carbon dioxide concentrations on the metamorphosis, size, and survival of larval hard clams (*Mercenaria mercenaria*), bay scallops (*Argopecten irradians*), and eastern oysters (*Crassostrea virginica*). Limnol Oceanogr 54: 2072–2080

Talmage SC, Gobler CJ (2010) Effects of past, present, and future ocean carbon dioxide concentrations on the growth and survival of larval shellfish. Proc Natl Acad Sci USA 107:17246–17251

Thompson PA, Montagnes DJS, Shaw BA, Harrison PJ (1994) The influence of three algal filtrates on the grazing rate of larval oysters *Crassostrea gigas*, determined by fluorescent microspheres. Aquaculture 199:237–247

Timmins-Schiffman E, O'Donnell MJ, Friedman CS, Roberts SB (2013) Elevated pCO_2 causes developmental delay in early larval Pacific oysters, *Crassostrea gigas.* Mar Biol 160:1973–1982

Vandenberg JI, Metcalfe JC, Grace AA (1994) Intracellular pH recovery during respiratory acidosis in perfused hearts. Am J Physiol Cell Physiol 266:C489–C497

Vargas CA, de la Hoz M, Aguilera V, San Martín V and others (2013) CO_2-driven ocean acidification reduces larval feeding efficiency and changes food selectivity in the mollusk *Concholepas concholepas.* J Plankton Res 35: 1059–1068

Vargas CA, Aguilera VM, San Martín V, Manríquez PH and others (2015) CO_2-driven ocean acidification disrupts the filter feeding behavior in Chilean gastropod and bivalve species from different geographic localities. Estuaries Coasts 38:1163–1177

Waldbusser GG, Brunner EL, Haley BA, Hales B, Langdon CJ, Prahl FG (2013) A developmental and energetic basis linking larval oyster shell formation to acidification sensitivity. Geophys Res Lett 40:2171–2176

Waldbusser GG, Hales B, Langdon CJ, Haley BA and others (2015a) Saturation-state sensitivity of marine bivalve larvae to ocean acidification. Nat Clim Change 5: 273–280

Waldbusser GG, Hales B, Langdon CJ, Haley BA and others (2015b) Ocean acidification has multiple modes of action on bivalve larvae. PLOS ONE 10:e0128376

Walther K, Anger K, Pörtner HO (2010) Effects of ocean acidification and warming on the larval development of the spider crab *Hyas araneus* from different latitudes (54° vs. 79° N). Mar Ecol Prog Ser 417:159–170

Widdows J, Newell RIE, Mann R (1989) Effects of hypoxia and anoxia on survival, energy metabolism, and feeding of oyster larvae (*Crassostrea virginica*, Gmelin). Biol Bull 177:154–166

Yan X, Zhang Y, Huo Z, Yang F, Zhang G (2009) Effects of starvation on larval growth, survival, and metamorphosis of Manila clam *Ruditapes philippinarum.* Acta Ecol Sin 29:327–334

Editorial responsibility: Myron Peck, Hamburg, Germany

Submitted: May 26, 2016; Accepted: November 7, 2016
Proofs received from author(s): December 15, 2016